Astron. Astrophys. 333, 205–218 (1998)

ASTRONOMY
AND
ASTROPHYSICS

Photospheric and chromospheric activity in the late-type giant component of the evolved binary system HD 185510⋆

A. Frasca, E. Marilli, and S. Catalano

Osservatorio Astrofisico di Catania, Viale A. Doria 6, I-95125 Catania, Italy

Received 6 November 1997 / Accepted 2 January 1998

Abstract. UBV photometry and moderate resolution Hα spectrophotometry of the evolved binary system HD 185510 (sdB + K0 III), performed at Catania Astrophysical Observatory, is presented and discussed. The spectrophotometric data were collected in 1991, 1993, and 1994, while the photometric light curves were obtained in 1993, 1994 and 1995.

From the B and V photometry we determine a new photometric rotational period of $26^d.23$, confirming the asynchronous rotation of the cool giant component. The spectroscopic data confirm the $v \sin i$ value of 15 Km s^{-1} measured by Fekel et al. (1993) and clearly reveal a filled-in Hα line with appreciable variations. The excess emission of the line, observed at any orbital phase, is found to be anticorrelated with the V light curve and is primarily ascribed to the chromospheric activity on the cool star.

The primary total eclipse is clearly visible in the U band, but undetectable in the V band. From the U observations we determined a total duration of the primary eclipse (from 1^{st} to 4^{rd} contact) of $1^d.3883$, with the ingress lasting only 27 minutes. This new accurate monitoring and timing of the eclipse allowed us to improve the system solution which leads to $R_C = 8.8\,R_\odot$, $T_C = 4800$ K, $R_H = 0.11\,R_\odot$, $T_H = 30\,000$ K for the cool and hot star respectively.

The evolution of HD185510B is discussed also in relation to the evolutionary status of HD 185510A and the synchronization time scale. HD 185510B is probably a sdB near the zero age extended horizontal branch, resulting from an enhanced mass loss in late case B or case A mass exchange with a possible common envelope phase. A small amount (15-20%) of mass loss from the system which can account for the strong IR excess is suggested.

Key words: stars: activity – binaries: eclipsing – subdwarfs – stars: individual: HD 185510

Send offprint requests to: A. Frasca (afrasca@astrct.ct.astro.it)

⋆ The complete U B V photometric data set is available in electronic form at the CDS via anonymous ftp to cdsarc.u-strasbg.fr or via http://cdsweb.u-strasbg.fr/Abstract.html

1. Introduction

HD 185510 (= V1379 Aql) is a binary system composed of a red giant star (K0 III) and an evolved hot subluminous star (sdB). The first indication of chromospheric activity on the giant star came from the detection of Ca II H & K emission (Bidelman & MacConnell 1973). A strong emission in the cores of the Ca II H & K lines, comparable to the more active RS CVn binaries, and an extremely weak Hα line has been reported by Fekel & Simon (1985).

Photometric variations with an amplitude of about $0^m.2$ were first observed by Henry et al. (1982). The behavior of the photometric wave was better defined by Lloyd Evans & Koen (1987) while Balona et al. (1987) discovered the eclipse of the subdwarf from the variation of about $0^m.12$ in the U–B color index.

The system is asynchronous, the rotational period of 25.4 days found by Balona et al. (1987) being longer than the orbital period (20.66 days) determined from radial velocity measurements (Balona 1987, Fekel et al. 1993). Hooten & Hall (1990) determined a photometric period of about 26 days with a variation amplitude of $0^m.20$–$0^m.25$ in the V band. In some seasons, they found that a smaller amplitude ($0^m.1$) light curve with a period of 13 days would better represent the data, but they suggested that such light curve results from a configuration of two-spot groups laying on opposite hemispheres of the active star.

The presence of a hot companion was noticed by Fekel & Simon (1985) in ultraviolet IUE spectra. From the flux distribution they derived an effective temperature of 20 000–30 000 °K for the hot star that was classified as a B type subdwarf. Jeffery et al. (1992) measured the radial velocity of the hot component in two high resolution IUE spectra taken at quadratures. Combining the radial velocity curves of both stars, they deduced a mass ratio $M_C/M_H \simeq 7.45$, and estimated masses of 2.3–2.8 $M_\odot$ for the K star and 0.31–0.37 $M_\odot$ for the hot star. On the basis of the eclipse light curve and the spectral energy distribution from the UV to the red, they derived effective temperatures of $T_H = 25\,000$°K, and $T_C = 4000$°K for the hotter and cooler component respectively. The mass of 0.31–0.37 $M_\odot$, which is lower than the typical value of sdB (Heber et al. 1984), and its higher gravity leads Jeffery et al. (1992) to conclude that

HD 185510B is not a true sdB, but, presumably, a star in the lower part of the Helium main sequence, or it is becoming a Helium white dwarf.

From a new radial velocity curve for the cool component, Fekel et al. (1993) significantly improved the orbital elements and the spectroscopic ephemeris. They also give a value of 15 ± 2 Km s^{-1} for the $v \sin i$ of the cool star, constraining the radius to 7.5-8 $R_\odot$. In addition, Fekel et al. (1993) discussed the characteristics of HD 185510 and other chromospherically active systems with hot compact companions in the context of the barium star scenario. They conclude that due to the short orbital period (small orbit size) the mass transfer in HD 185510 occurred before the mass donor reached the phase where the s-process elements could be transferred to the surface, consistent with the lack of abundance anomalies in the cool component of the system.

While this paper was nearly completed, a paper on the analysis of the eclipse based on UV observations with IUE was published by Jeffery & Simon (1997).

In order to reconcile the results from the eclipse solution and the gravity derived from the Ly α profile of the subdwarf component, they claim that the ingress/egress profile is affected by eclipse from the cool star atmosphere. They deduced $T_{\rm eff} = 31\,500$°K and $\log g = 7.3$ from the Ly α profile and the CII,III and SiII,III ionization equilibrium, while the radius inferred from the eclipse analysis leads to $\log g = 6.5$.

The scale height $h = 0.034\ r_{\rm P}$ of the optical depth they deduce from the solution of the light curve at $\lambda = 1400$ Å is significantly larger than that of the supergiant HR 6902A (ζ Aurigae) and Arcturus, both of $\log g = 2$ (Schröder et al. 1996). Since HD 185510A has $\log g = 2.9$, the atmosphere height should be coherently smaller. Moreover the shorter ingress observed at $\lambda = 1800$ Å and the smaller scale height of only 0.012 $r_{\rm P}$ they derived at this wavelength is inconsistent with the expected optical depth at the two observation bands. In fact the linear absorption coefficient at 1800 Å is smaller than at 1400 Å at least by a factor of ten (Travis & Matsushima 1968, Dragon & Mutschlecner 1980) and therefore the optical depth scale height should be ten times larger implying a longer duration of the atmospheric eclipse.

The resolution time of Jeffery & Simon (1997) observations (19 min) is very close to ingress/egress duration so that, with observations of only one eclipse, they can hardly define the real eclipse duration and the light curve profile, therefore their argumentation on the atmospheric eclipse should be taken with some caution.

We have observed 4 eclipses ingresses and egresses in the U band with an average time resolution of 40 sec. With these data we should be able to settle the problem of the atmospheric eclipse and accurately determine the radius and therefore the gravity of the secondary hot component.

In the following we present photometric and spectroscopic Hα observations of HD 185510 and discuss them in terms of activity at the surface of the cool giant component. On the grounds of the new light curve solution we will discuss a possible scenario for the evolutionary stage of the system.

Table 1. Magnitudes and colors of the comparison and standard stars

HD	V	B–V	U–B
185567 (c)	8.321	0.620	0.169
185587 (ck)	9.089	0.182	-0.019
184573	6.330	1.120	0.920
185124	5.450	0.430	0.000
188405	6.500	0.390	0.030
190172	6.710	0.350	0.004

2. Observations and data reduction

2.1. Photometry

The photometric observations have been carried out in the standard UBV system with the 91-cm Cassegrain telescope at the *M. G. Fracastoro* station (Serra La Nave, Mt. Etna) of the Catania Astrophysical Observatory. The observations were performed with a photon-counting cooled photometer equipped with an EMI 9789QA photomultiplier. We observed HD 185510 on only two nights in 1991, on 16 nights in 1993, on 19 nights in 1994 and 28 nights in 1995, covering several orbital cycles.

HD 185567 and HD 185587 were used as comparison and check stars, i.e. the same stars adopted by Henry et al. (1982). Lloyd Evans et al. (1983) indicated that the comparison star HD 185567 could be variable, however magnitude differences against the check star do not show variability within $0^m.015$ along all our observing runs.

Field stars of known magnitudes and colour indices were observed nightly to transform the instrumental magnitudes to the Johnson photometric system. Magnitudes in the V band and color indices of the standard and program stars are given in Table 1.

2.2. Spectroscopy

Spectroscopic Hα observations were also performed at the *M. G. Fracastoro* observing station of Catania Astrophysical Observatory using the REOSC echelle spectrograph both in the low and high dispersion mode. The spectra were recorded on a 385×576 pixel E.E.V. CCD of 22×22 μm pixel size (Bonanno & Di Benedetto 1990). Low dispersion spectra, with an instrumental resolution of 0.89 Å/pixel (see Frasca & Catalano, 1994), were obtained in 1991 on 8 nights from July 31 to August 11, i.e. about 2/3 of the orbital period and on 3 nights in August 1993; these and the subsequent observations were made with the spectrograph connected to the telescope through an optical fiber link. In 1994 we acquired five spectra with the echelle spectrograph used in cross-dispersion configuration, which gives an instrumental resolution of 0.22 Å/pixel. The spectral resolution of about 0.46 Å, deduced from the full width half maximum of the Th-Ar calibration lamp emission lines, corresponds to a two-pixel sampling. The spectra were taken with typical exposure times of 20–25 min, so that a signal-to-noise ratio (S/N) of

90–120 for the low resolution spectra and about 50–60 for the high-resolution ones was reached at the Hα continuum.

The low resolution spectra were extracted from the CCD images following a standard reduction procedure, written in the IDL (Interactive Data Language) environment, whose steps are described in Frasca & Catalano (1994). The reduction of the high resolution echelle spectra was performed using the Image Reduction and Analysis Facility (IRAF [1]) package of NOAO. During each observing season, two non-active stars (91 Aqr and ϵ Cyg) of the same spectral type (K0 III) as the active star in the system were observed. These standard star spectra were acquired to reproduce the photospheric Hα profile of the chromospherically active component, so that, by making the difference between the observed and the synthetic spectrum, we were able to isolate the chromospheric emission in the line. The method of constructing the synthetic spectrum is described in Frasca & Catalano (1994). Since the contribution of the subdwarf to the observed spectrum in the red side of the visible region is negligible, we only subtracted the spectrum of a standard K0 III star from each observed spectrum of HD 185510. We used 91 Aqr in 1991 and ϵ Cyg in 1994 as standard stars. The higher resolution of the 1994 spectra allowed us to detect the rotational broadening of the cool component of HD 185510, therefore the spectrum of ϵ Cyg was convolved with a rotational profile (Gray 1992) of $v \sin i = 15$ Km s^{-1} (Fekel et al. 1993), adopting a limb darkening coefficient $\mu = 0.7$ typical of a K0 giant star at these wavelengths (Gray 1992).

The net Hα emission equivalent width ($W_{\rm H\alpha}$) has been measured integrating the resulting emission profile in the difference spectra (see Fig. 8–9). The error $\Delta W_{\rm H\alpha}$ in the net equivalent width has been evaluated by multiplying the integration range to the photometric error on each point. This latter has been estimated by the standard deviation of the observed flux values on the difference spectra in two line-free spectral regions near the Hα.

The use of two different standard stars, nominally of the same spectral type, in the two observing sessions could introduce a systematic difference in the $W_{\rm H\alpha}$ values, but this contribution, as discussed by Frasca & Catalano (1994), should be $\leq$ 0.05 Å. Another source of systematic differences between the two data sets, presumably of the same order of magnitude, could be introduced by the different spectral resolution, and by the different set-up of the spectrograph. The good agreement between the two data sets seems to confirm these error estimates.

[1] IRAF is distributed by the National Optical Astronomy Observatories, which is operated by the Association of Universities for Research in Astronomy, inc. (AURA) under cooperative agreement with the National Science Foundation.

3. Results

3.1. Photometry

3.1.1. The orbital period

Our photometric observations span several orbital periods and all together give a complete coverage of the eclipse both at total and partial phases.

The egress observed on 1995 Aug 16 (JD = 2449946.41) is the only well covered egress up to now and has allowed us to define with very good accuracy the total duration of the eclipse, putting a strong constraint on the cool star radius when an independent guess on the system inclination is made. Combining all our observations with Jeffery et al. (1992) and Jeffery & Simon (1997) data of the eclipse ingress and egress, we have established an accurate time of mid eclipse and of the period, thus deriving the following ephemeris:

$$HJD_{\rm mid-ecl.} = 2449656.4804 \pm 0.0015 + (20^d.66118 \pm 0^d.00005) \times E \quad (1)$$

This orbital period is a little bit shorter than the period of 20$^{\rm d}$.6619 derived by Fekel et al. (1993) for the spectroscopic orbit. Using this ephemeris the predicted eclipse date of 2446577.954 is only 4^m later than deduced by Fekel et al. (1993), i.e. in excellent agreement.

3.1.2. Rotational modulation

Due to the small size of the secondary hot star, no photometric eclipse is detectable in the V band, so that the observed variation can be due to the rotational modulation of K star and reflection effect. As pointed out by previous authors, the system is asynchronous (Balona et al. 1987, Hooten & Hall 1990), therefore these variations should follow different periodicities. The photometric B and V data distributed over different orbital cycles have been analysed applying the periodogram technique (Scargle 1982). The CLEAN iterative deconvolution algorithm (Roberts et al. 1986) has been used to eliminate the effects of the data sampling introduced by the observation spectral window in the power spectrum. The V data sets for the 1993, 1994 and 1995 have been separately analysed leading to rotational periods of 26$^{\rm d}$.49$\pm$1.9, 26$^{\rm d}$.94$\pm$3.3, and 26$^{\rm d}$.28$\pm$2.1 respectively. The cleaned periodograms for the three data sets displayed in Fig. 1 do not show evidence of peaks at the orbital-period frequency, indicating that no detectable eclipse or reflection effect is present. On the other hand, due to the large geometrical dilution factor, the irradiated side of the cool star would be warmed by less than 10 K. The U magnitudes proved not useful for the rotational analysis because of the eclipses, whose occurrence at different rotational phases produces a peak at the orbital period frequency as additional disturbing periodicity.

The rotation periods independently estimated for the three data sets agree with each other within the errors. The shape of our light curves is quite different in the three observational seasons, as can be seen from Fig. 2 in which the B and V light

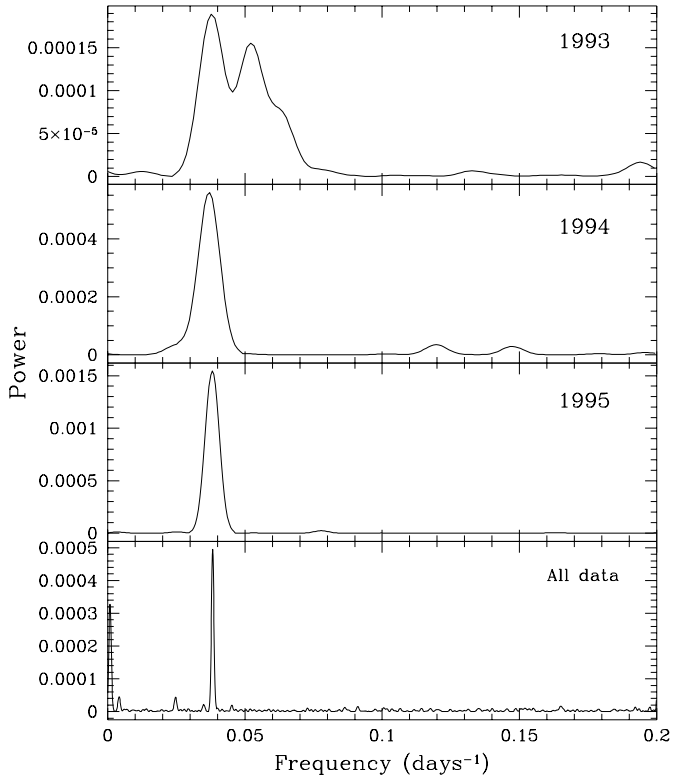

Fig. 1. Periodograms for the 1993, 1994 and 1995 data sets.

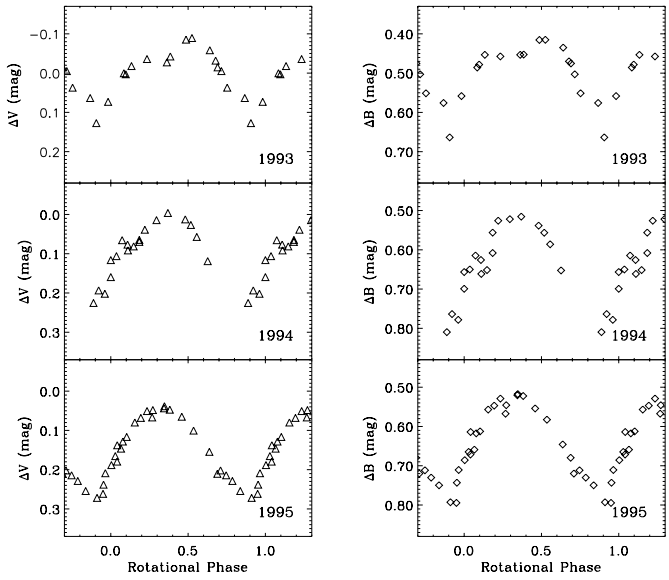

Fig. 2. V and B light curves folded with the yearly periods but time of minimum reckoned from the ephemeris in relation 2. Magnitude differences are referred to the comparison star HD 185567.

curves are presented folded with the yearly periods of $26^{\rm d}.49$, of $26^{\rm d}.94$ and $26^{\rm d}.28$.

However, in order to improve these estimates we have computed the period from all the data sample, assuming that no significant variation in the longitude of the active region occurred during all the observations. In principle, we should have a much better determined period, because more rotational cycles are covered. The periodogram peak becomes sensibly narrower leading to a period of $26^{\rm d}.16\pm0.36$, which is a little shorter than the rotation periods derived for the single years. This suggests that, on the average, the active longitude belt is maintained during a time-scale of at least three years and only very local redistribution of the spots does occur, as indicated by the change in the light curve amplitude.

The average period found from our observations is significantly longer than the value of 25.4 days derived by Lloyd Evans & Koen (1987) and the 25.7 days found by Hooten & Hall (1990). This could be indicative of a steady increase of the rotation period with time. Since it would lead to a spin down time scale too short to be accounted for by any reasonable physical process (magnetic brake normally follows a square root dependence on the age (Skumanich 1972, Catalano et al. 1988); tidal effects forcing co-rotation, although improbably due to the large separation, should lead to a decrease of the rotation period, because the orbital period is shorter than the rotation one) we have investigated whether these apparent changes could result from erratic variations around some average period.

Independent linear fits to the time of maximum and minimum light, determined from the original observations available in the literature, lead to a mean rotation period of 26.2342 days. The shape of the minima is better defined in all light curves, and their timing leads to O–C values generally smaller than 1 day, which are well within the uncertainties of the determinations, also taking into account the errors introduced by the changes in the light curve asymmetry. However the average time of the minimum at JD=2444803.0 deduced from Lloyd Evans & Koen (1987) observations gives an unreasonable O–C $\simeq 6$ days (Fig. 3). Considering that the time of minimum at JD=2445139.26 taken from Henry et al. (1982) observations agrees very well with all other minimum times, there is no way to reconcile Lloyd Evans & Koen (1987) minimum time with the other ones. Thus, adopting the time of minimum in Hooten & Hall (1990) data as reference, one of the best observed, we deduce the following ephemeris for the rotation of the K0 component of HD 185510.

$$JD_{hel} = 2447315.826 + 26.2342 \times E \qquad (2)$$

3.1.3. Light curve solution

The eclipse determines a decrease of light of $\simeq 0^m.14$ in the U band, but it is not immediately possible to superimpose one to the other different eclipses because of the asynchronism between the rotational period of the K0 III star and the orbital one. This effect is much more reduced in the U–B color index, which displays only very small amplitude variations with the rotation of the star. The eclipse depth we found in this color index Δ(U–B) $\simeq 0^m.12$ substantially confirms the value found by Balona et al. (1987).

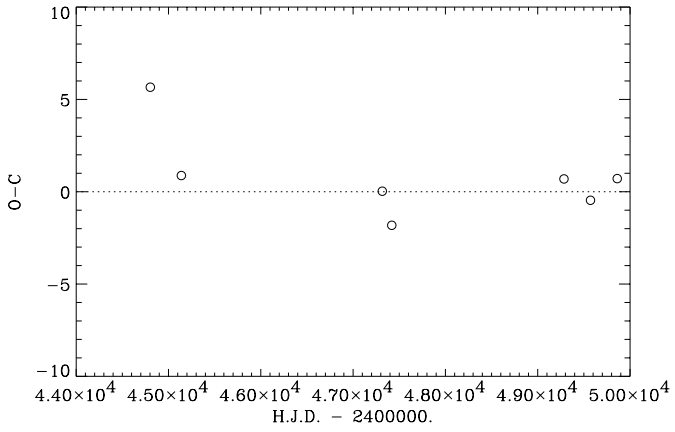

Fig. 3. O–C of the time of V light minimum with respect to the ephemeris JD_{hel} = 2447315.826 + 26.2342 × E

The U and B nightly averaged magnitudes of 1995 folded with the rotational period of $26^{\rm d}.28$ displayed in Fig. 4 clearly show that the in-eclipse points are systematically lower than the out-of-eclipse ones, and represent the intrinsic variation of the K star. It appears also that the amplitude of the light curve is larger for the in-eclipse data (solid symbols) than for the out-of-eclipse data (empty symbols), because of the different weight of the secondary hotter star in the combined light of the system at the different rotational phases.

In order to find a solution of the light curve, to derive the elements of the system, we need to remove the rotational modulation from the data, and re-normalize the eclipse depth to the unspotted hemisphere of the secondary star.

To obtain the clean orbital light curve we proceeded in the following way. Defining $\gamma = \frac{L_{\rm H}}{L_{\rm C_{max}}}$ as the ratio of the subdwarf to the giant luminosity at the rotational light maximum (minimum spot visibility), we can express the rotational magnitude variation of the giant only, normalized to its wave maximum, $\Delta m_{\rm cool}(\phi)$, in terms of system magnitude (hot + cool) $\Delta m_{\rm sys}(\phi)$, normalized to the maximum of the combined light

$$\Delta m_{\rm cool}(\phi) = -2.5 \log \left(\frac{L_{\rm C}(\phi)}{L_{\rm C_{max}}} \right)$$
$$= -2.5 \log \left(\gamma \left(10^{-0.4 \Delta m_{\rm sys}(\phi)} - 1 \right) + 10^{-0.4 \Delta m_{\rm sys}(\phi)} \right) \quad (3)$$

Since from the in-eclipse observations we determine the magnitude of the K star at the various rotational phases (first member of relation 3), we should be able to obtain γ and therefore normalize the light curve to the unspotted hemisphere luminosity. First we express the asymmetric light curve outside the eclipse by means of a periodic function of the type

$$\Delta m_{sys}(\phi) = a_0 + a_1 \sin(2\pi\phi + \Phi_1) + a_2 \sin(4\pi\phi + \Phi_2) \quad (4)$$

where ϕ is the rotational phase. Then, inserting the fitting function $\Delta m_{\rm sys}(\phi)$ in the relation 3 we obtain the rotational variation of the K star $\Delta m_{\rm cool}(\phi)$ (dashed line in Fig. 4) for the appropriate value of γ to be compared with the observed magnitude

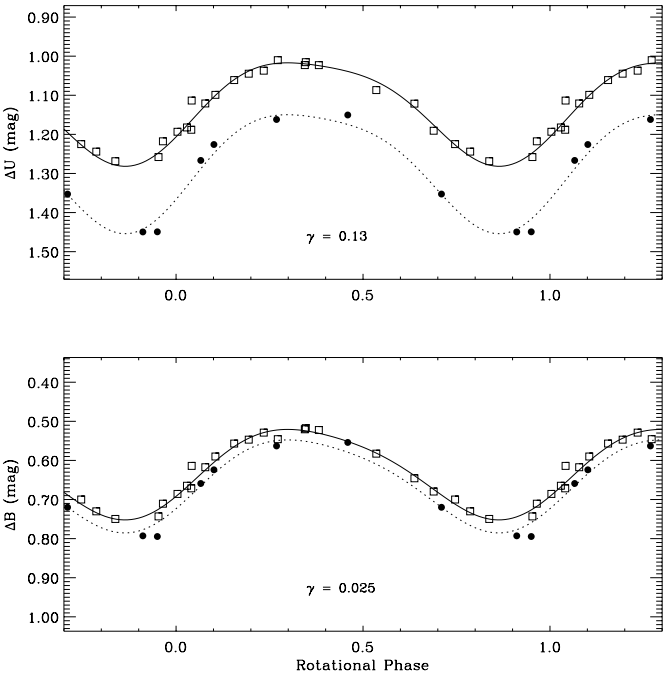

Fig. 4. U and B 1995 nightly averaged magnitudes folded with the rotational period. Open squares represent out-of-eclipse data, filled circles indicate in-eclipse magnitudes. The solid line is a fit of a periodic function to the out of eclipse data. The dotted line is the same fit scaled to the in-eclipse points, with the adopted luminosity ratio, γ.

at totality. By trial and error, through an iterative process, we find for the 1995 data γ = 0.13 for the U and γ = 0.025 for the B light curve. The same procedure has been applied to the 1994 U and B data with a similar result.

The γ values that we derive are correlated to the ΔU and ΔB eclipse depths through the following relation

$$\Delta m_{ecl} = -2.5 \log \frac{L_{\rm C_{max}}}{L_{\rm C_{max}} + L_H} = 2.5 \log(1+\gamma) \quad (5)$$

The wave-corrected light curve has been derived by dividing the observed luminosities by the fit curve. In this way the corrected magnitudes outside the eclipse are set to zero, while the level of the U points at totality defines the eclipse depth relative to the maximum light (minimum visibility of spots) of the K0 III star, which leads to depth values of $0^m.134$ and $0^m.027$ for the U and B filters respectively.

The portion of the renormalized light curve at a phase interval around the eclipse is reported in Fig. 5. Observations at the egress reflected around the centre of the eclipse have been superimposed with different symbols. From Fig. 5 the eclipse appears symmetric, i.e. the ingress and egress occur with the same duration of about 27 minutes (0.00090 in orbital period units) which is significantly shorter than the upper limit of about 1 hour ($0^{\rm P}.0022$) estimated by Jeffery et al. (1992) on the basis of IUE FES and UBV photometry, and is in excellent agreement with the mean value ($0^{\rm P}.00092$) quoted by Jeffery & Simon (1997). The duration of the totality (from the $2^{\rm nd}$ to the $3^{\rm rd}$ contact) is $1^{\rm d}.3512$, corresponding to $0^{\rm P}.0654$, while the total

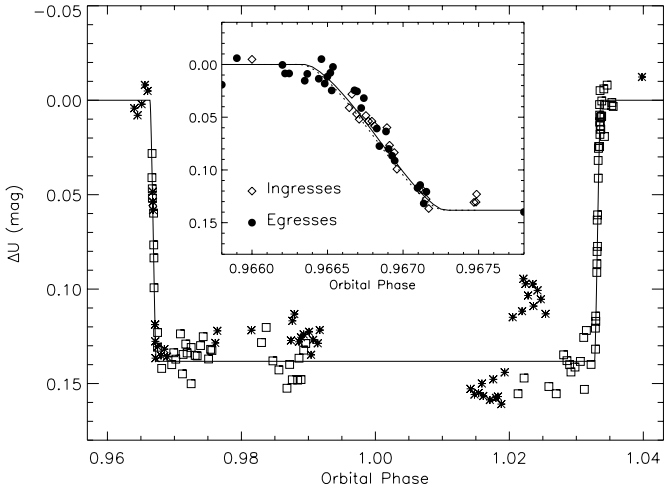

Fig. 5. Observations of the eclipse in the U filter in 1994 (asterisks) and 1995 (squares) and light curve solution (full line). In the inset the ingress (diamonds) reversed egress (filled circles) and the light curve solution (full line) are displayed. The dotted line, barely visible in the figure, represents the light solution taking into account the atmospheric eclipse.

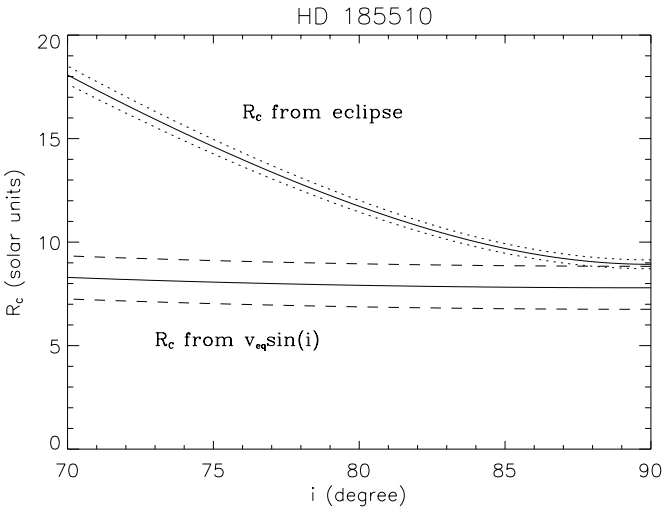

Fig. 6. The radius of the cool giant component $R_{\rm C}$ as derived from the eclipse solution relation(Eq. 7) and from $v \sin i$ (Eq. 8) is plotted against the orbital inclination. The dotted and dashed curves are the limiting bounds to the $R_{\rm C}(i)$ relations defined by the errors in $a \sin i$ and $v \sin i$.

duration (from the 1$^{\rm st}$ to the 4$^{\rm th}$ contact) of 0$^{\rm P}$.0672$\pm$0.0001 is consistent with the value of 0$^{\rm P}$.0678$\pm$0.0015 already quoted by Jeffery et al. (1992), and in excellent agreement with the value of 0$^{\rm P}$.06755 by Jeffery & Simon (1997).

Since only the primary eclipse is observable, it is not possible to deduce from the light curve all the three parameters $R_{\rm H}$, $R_{\rm C}$, and i. Then an independent determination of at least one of these three parameters is needed.

The distance δ between the centers of two eclipsing spherical stars (in units of the system separation) as a function of the orbital phase ϕ is given by (Kopal 1959)

$$\delta^2 \; = \; \cos^2 i \; + \; \sin^2 i \; \sin^2(2\pi\phi) \qquad (6)$$

Since the ingress/egress duration is much shorter than the total duration of the eclipse, i.e. the secondary hotter star is much smaller than the primary, at the third contact we approximately have $\delta \; \simeq \; R_{\rm C}/a$ and therefore

$$R_{\rm C} \; \simeq \; \frac{(a \sin i)}{\sin i} \sqrt{\cos^2 i \; + \; \sin^2 i \; \sin^2(\pi \Delta\phi_{\rm T})} \qquad (7)$$

where $(a \sin i)$ is the projected semi-major axis of the relative orbit and $\Delta\phi_{\rm T} \; = \; 0.0663$ the duration of the eclipse from half ingress to half egress. The radius of the star can be also expressed in terms of the measured $v \sin i$ and of the rotation period as:

$$R_{\rm C} \; = \; \frac{P_{\rm rot}}{2\pi} \frac{(v \sin i)}{\sin i} \qquad (8)$$

The values of $\rm R_C$ derived by Eq. 7 and Eq. 8 adopting $v \sin i \; = \; 15 \pm 2$ Km s^{-1} and a sin i =30.05 10^6 km (Fekel et al. 1993) and our rotational period of 26$^{\rm d}$.23 are plotted as a function of the system inclination in Fig. 6. The dotted and dashed lines represent the limiting bounds to the $R_{\rm C}(i)$ relations from Eq. 7 and Eq. 8 defined by the errors in $a \sin i$ and $v \sin i$ determinations.

As can be seen in Fig. 6 the superposition region in the plane $R_{\rm C}$–i is very near to 90°, and only for the upper limit of $v \sin i$, which leads to $R_{\rm C} \; = \; 8.83 R_{\odot}$. We therefore assume for our subsequent discussion $i \; = \; 90°$ and $R_{\rm C} \; = \; 8.8 \; \pm \; 0.2 \, R_{\odot}$.

In the uniform discs approximation (no atmospheric eclipse) the radius of the sdB star is given by

$$R_{\rm H} \; = \; \pi \frac{(a \sin i)}{\sin i} \Delta\phi_{\rm i} \sqrt{1 - \frac{\cos^2 i}{\pi^2 \Delta\phi_{\rm T}^2 + \cos^2 i}} \qquad (9)$$

where $\Delta\phi_{\rm i} \; = \; 0.00090$ is the phase interval of the ingress which, for $i \; = \; 90°$, gives $R_{\rm H} \; = \; \pi \frac{(a \sin i)}{\sin i} \Delta\phi_{\rm i} \; = \; 0.12 R_{\odot}$.

Because of the absence of the eclipse in the V band, and the very modest eclipse depth in B light the analysis of the system is only possible with the U light curve. Therefore, in order to reach a more accurate determination of $R_{\rm H}$, $R_{\rm C}$ and of effective temperatures we have fitted a theoretical light curve to our normalized U data.

The eclipse depth in the U filter is related to the ratio of U luminosities of the components, which in turn depends on radii and surface fluxes, i.e. on effective temperatures. However in the case of HD 185510A the flux distribution is neither coherently defined by current spectral type nor by color indices versus effective temperature calibrations. The spectral type classification K0 III/IV (Bidelman & Mac Connel 1973) or the color index B–V = 1.16 at totality would lead to a temperature of 4 800 °K (Bell & Gustaffson 1989) and 4 420 °K (Schmidt-Kaler 1982) respectively. Moreover the B–V index is at odds with the spectral type, suggesting some degree of reddening with $\rm E_{B-V}$ =0.16. Such a value of color excess is unreasonably larger than expected for a normal interstellar reddening (at a distance of 235$\pm$61 pc we

expect $E_{B-V} \sim 0.077 \pm 0.02$) and barely consistent with the UV spectrum analysis of the hot component (Jeffery & Simon 1997). The observed U–B = 0.85, is appropriate for a K0 III star. Although some part of this apparent excess may be due to interstellar or circumstellar reddening, there is evidence that active stars have anomalous colour indices with respect to normal inactive ones. Fekel et al. (1986) found chromospherically active stars to have red color indices significantly redder than inactive stars. At near-IR wavelengths the observations of RS CVn systems have produced conflicting results; some authors do not find significant IR excess (Antonopoulou 1983, Antonopoulou & Williams 1984, Berriman et al. 1983) while others argue in favour of its presence (Hall et al. 1975, Milone 1976, Verma et al. 1983). However Busso et al. (1988), using IRAS observations showed that some sources appear to have large IR excess, while some others do not. Actually HD 185510 was found to have the largest IR excess [(V–12μ) = 1.2 mag] among the stars of their sample.

On the other hand Amado & Byrne (1996), analysing the effect of activity on the $(U–B)_0$ v.s. $(B–V)_0$ colour–colour diagram, show that for single-lined spectroscopic RS CVn systems there exists an ultraviolet excess with respect to that of quiescent stars of the same spectral type. The effect is found to be related to the level of activity as measured by the X-ray emission, and white-light faculae are indicated as reasonable candidates for the UV excess.

The U–B and B–V colours of HD 185510, even after the correction for interstellar extinction, lay above the mean zero-reddening curve, thus indicating a positive UV excess, as found for the majority of RS CVn giants by Amado & Byrne (1996).

Jeffery & Simon (1997), from a revised analysis of the out-of eclipse flux distribution, propose for the K0 star a $T_{eff} = 4500 \pm 300$ K and found the spectrum to be metal-deficient.

However, in order to get rid of this complicated situation of the secondary star with UV excess on one side and IR excess on the other, possibly indicating circumstellar matter, we have avoided the use of model atmosphere to estimate the flux and luminosity of the K star.

We simply evaluated the U surface flux of the cool component by means of the observed U–V at eclipse and the estimated surface flux in the V band. The average V surface fluxes have been deduced using a sample of stars of different B–V, with measured angular diameters reported in literature (Barnes et al. 1978, Scargle & Strecker 1979, Blackwell & Lynas-Gray 1994).

The synthetic light curve has been computed through a routine developed in IDL, which calculates the light losses due to eclipses of spherical limb-darkened stars. We have performed three light curve fits, the first one using the observed in-eclipse values of B–V = $1^m.16$ and U–B = $0^m.85$, the second dereddening these values for a $E_{B-V} = 0.05$ and the third considering a $E_{B-V} = 0.10$, i.e. the maximum value attainable with the distance and a mean extinction law and compatible with the UV spectrum of the hot secondary (Jeffery & Simon 1997).

The solution produces the U surface flux of the hot component, which, interpolating in the Kurucz (1979) models for $\log g = 5$, yelds the effective temperature appropriate for this star. Unfortunately model atmospheres for the more appropriate value $\log g \approx 6$ are not available, but differences are expected to be very marginal.

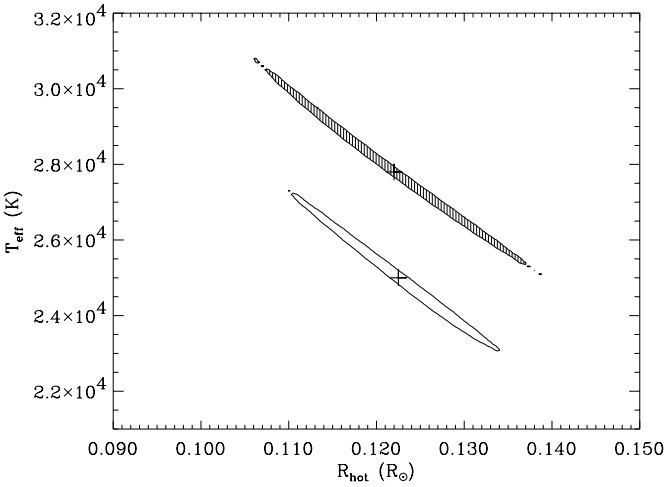

Fig. 7. Confidence regions at 80 % probability level for the χ^2 of the eclipse light curve fit. The dashed region is for the value of $E_{B-V} = 0.10$, the lower empty region is obtained fixing $E_{B-V} = 0.05$.

The χ^2 of the light-curve fit is calculated as a function of the radius and effective temperature of the hot subdwarf, fixing the color excess. The contours of regions with a confidence level of 80 % for χ^2 are displayed in Fig. 7. The dashed region corresponds to solutions with $E_{B-V} = 0.10$ ($U–V_{cool} = 1.84$) for which a $R_H = 0.122 \pm 0.015\ R_\odot$ and $T_H = 27\,800 \pm 2500$ K are deduced as the best solution. The empty contour relates to the solution with $E_{B-V} = 0.05$ ($U–V_{cool} = 1.92$) which gives $R_H = 0.1225 \pm 0.0115\ R_\odot$ and $T_H = 25\,000 \pm 2000$ K as the best solution.

Following the suggestion of Jeffery & Simon (1997) of possible atmospheric eclipse produced by the external layers of the cool giant, we have investigated if such a phenomenon could affect the ingress shape and duration leading to an overestimate of the subdwarf radius. First we have computed the optical depth τ_ν for the atmosphere of the cool giant for three wavelengths ($\lambda\lambda$ 1400, 1800, 3600 Å) by means of the model atmosphere code ATLAS (Kurucz 1979), adopting $\log g = 2.9$, $T_{eff} = 4800°$K. The optical depth scale height of the more external layers come to be ≈ 1 200 km, 1 500 km and 26 000 km for the three wavelengths respectively. This result rules out any possibility of atmospheric eclipse at least at the UV wavelengths, contrary to the suggestion of Jeffery & Simon (1997). Since the optical depth scale height for the U band (λ = 3600 Å) is not completely negligible with respect to the hot star radius we computed the eclipse light curve including the atmospheric effect. The model calculation uses the τ_ν distribution with height from Kurucz model atmosphere. As indicated by the eclipse light curve (dotted line in the inset of Fig. 5) the effect of the atmosphere is negligible and the atmospheric eclipse phase would last only 2.3 min, i.e. about the 10 % of the ingress/egress duration and well within the uncertainties of our data. On the grounds of these considerations and on the basis of Jeffery and Simon

(1997) result for interstellar absorption, we propose as best solution that obtained for $E_{B-V} = 0^m.1$. However the comparison with the IUE UV spectrum does suggest an effective temperature near to the upper value allowed by the eclipse solution (i.e. $T_H = 30\,000$ K and $R_H = 0.110\ R_\odot$).

Therefore we propose the new elements of the system as reported in Table 2. The cool giant effective temperature is that appropriate for its spectral type K0 III (Bell & Gustaffson 1989).

3.2. Spectroscopy

The low resolution spectra, in the Hα region, are displayed in Fig. 8 together with the spectrum of the adopted standard star 91 Aqr (K0 III). The relevant filling-in of the Hα line and the variable residual emission profile can be seen on the right side of the figure. The spectra acquired in 1994 with a higher resolution (0.46 Å) and the differences with respect to the rotationally broadened spectrum of the reference star ϵ Cyg (K0 III) are shown in Fig. 9.

The net equivalent width values are reported in Table 3 together with the estimated error $\Delta W_{H\alpha}$, and are displayed in Fig. 10a and b folded with the orbital and rotational periods. The data of 1991, 1993, and 1994 are represented by different symbols. All together the Hα EW's display a variation amplitude of about 0.4 Å in 1991 and 0.7 Å in 1994. Although the data phased with the orbital period seem to show a regular trend, it is not easy to interpret their behaviour. Hα emission in systems with hot companions may show orbital modulation due to the reflection effect as in the case of FF Aqr (Marilli et al. 1995), therefore a sinusoidal behaviour with the maximum at phase $0^P.5$ and no emission at phase $0^P.0$ is expected. In the case of HD 185510 (lower panel in Fig. 10a and b) the Hα emission maximum occurs near phase $0^P.7$ and the minimum near phase $0^P.0$. However, the average emission equivalent width $W_{H\alpha} \simeq 0.6$ Å near phase $0^P.0$, indicates that a large part of the emission has a chromospheric origin.

The plot of the data vs. the rotational phase (upper panel in Fig. 10a and b) shows that the net Hα equivalent width is fairly well correlated with the photometric period. The Hα maximum falls near the 0.0 rotational phase and the Hα minimum is at $\phi_{rot} \simeq 0.4$, i.e. at the same rotational phases as the minimum and the maximum, respectively, of the B and V light curves from 1993 to 1995. This behavior is suggestive of a spatial association of photospheric and chromospheric active regions as observed in more typical RS CVn systems (Catalano et al. 1996). If this is the case, the Hα variations of HD 185510 would be mainly due to chromospheric inhomogeneities rather than to photoionizations induced by the subdwarf UV flux on the outer atmosphere of the cool K0 III companion as observed in FF Aqr (Marilli et al. 1995).

When folded with the rotational period of $26^d.2342$ and the photometric initial epoch HJD0 = 2447315.826, the 1991 data are in good agreement with the 1994 ones taken near the same rotational phases, therefore the lower resolution of 1991 data does not seem to influence significantly the results.

Table 3. Net Hα equivalent widths with their errors.

Hel. Jul. Day	Orbital Phase	$W_{H\alpha}$(Å)	$\Delta W_{H\alpha}$(Å)
2448469.38921	0.193	0.8690	±0.1042
8469.44477	0.195	0.8647	0.1235
8470.39693	0.228	0.8958	0.1355
8470.41776	0.229	0.7606	0.1506
8472.38249	0.298	0.9224	0.1034
8472.40958	0.299	0.9155	0.0889
8473.37632	0.332	0.8846	0.1462
8473.43952	0.335	0.7820	0.1014
8474.50834	0.372	0.8749	0.1071
8477.49745	0.476	0.6857	0.1009
8480.37682	0.577	0.7863	0.1336
8481.41856	0.614	0.4766	0.0860
9222.39843	0.522	0.5754	0.0536
9223.41933	0.558	0.6157	0.0493
9224.37772	0.591	0.6049	0.0668
9627.29146	0.679	0.7852	0.0853
9627.30638	0.680	0.8062	0.0564
9628.33848	0.716	0.8422	0.0615
9639.35380	0.101	0.5437	0.0649

The high Hα emission observed on 1994 September 27 may be related to an intrinsic activity variation, like a flare eruption. The corresponding Hα profile shows broad emission wings (more prominent on the blue side) which give rise to a stronger and wider net profile than those observed few days apart. Broadening of the Hα line wings has been frequently observed, during flares, in many RS CVn systems (Fraquelli 1984, Montes et al. 1996) and seems to be related to mass motion as observed in solar flares.

4. Discussion and conclusions

The primary K0 giant of HD 185510 has been found to be quite active both at photospheric and chromospheric level. Our light curves of the three years are asymmetric with the decrease from the maximum to the minimum steeper than the rise from the minimum to the maximum. However, the main feature is a hump just before the maximum clearly defined in the 1993 light curve, which gradually disappears in 1994 and 1995. A similar feature characterizes the Hooten & Hall (1990) light curve, while the asymmetry at the maximum appears reversed in Lloyd Evans & Koen (1987) observations. The change in the asymmetry is accompanied by a decrease in the maximum and minimum levels, and therefore in the mean magnitude. A similar behaviour is reported by Balona et al. (1987), who observed, in 1987, a $< \Delta V >$ magnitude mean level $0^m.05$ brighter than in the 1979–1981 session.

Mean parameters of present and previous light curves are reported in Table 4. A synthesis of the available V light curves of HD185510, grouped for homogeneous time intervals and authorship is shown in Fig. 11. The general behaviour of the light curves is characterized by a deep steady minimum at phase

Table 2. Physical elements of the two components of HD 185510 for $i = 90°$.

Star	Radius ($R_\odot$)	T_{eff} (°K)	L ($L_\odot$)	Mass* ($M_\odot$)	$\log(g)$
Cool	8.8 ±0.2	4 800	36.8	2.24 ±0.12	2.9
Hot	0.110 ±0.015	30 000 ±2 500	8.0 ±1.0	0.300 ±0.014	$5.83^{+0.11}_{-0.15}$

* from Fekel et al. (1993)

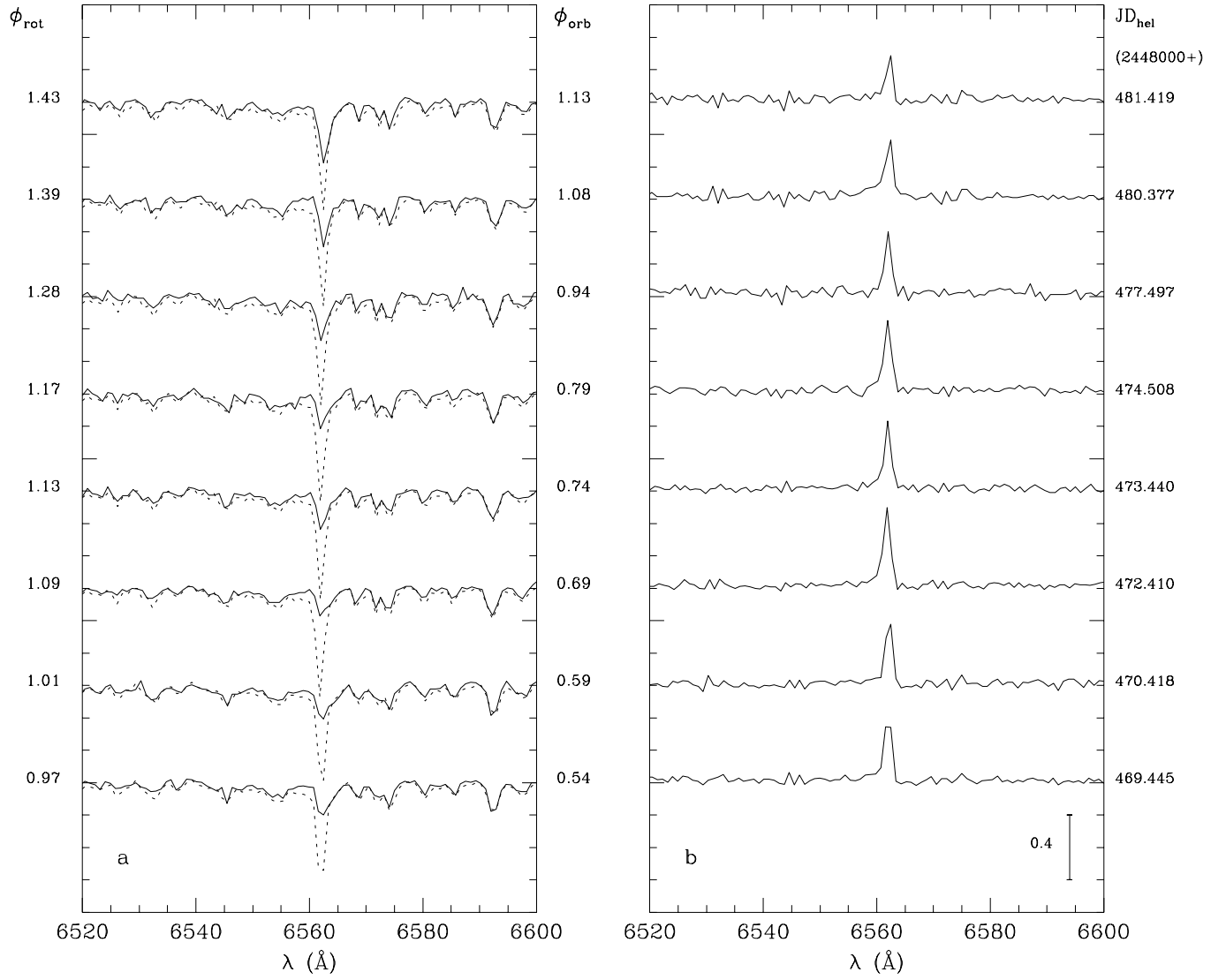

Fig. 8. **a** Hα spectra of HD 185510 in 1991 with superimposed the adopted standard 91 Aqr (dotted line). **b** Residual Hα emission.

$0.^P0$ and a variable feature around phase $0.^P5$ superimposed to the maximum light. In the currently accepted hypothesis that the light changes are due to unevenly distributed starspots on the K0 giant, the detection of a constant rotation period reveals the presence of a long lasting preferential active longitude, the main one more stable at phase $0.^P0$ and the variable one in the opposite hemisphere, which appears and disappears from time to time and moves also in longitude by about 70-90°.

Small changes in the spots distribution driven by differential rotation, decay and appearance of spots groups at different latitudes could account for the different rotation period in short time intervals and the phase shifts in some individual rotational light curve, the shift in the Lloyd Evans & Koen light curve phase being the most striking case.

The Hα emission shows a clear modulation with the rotation period (upper panel in Fig. 10a and b). The obvious anticorre-

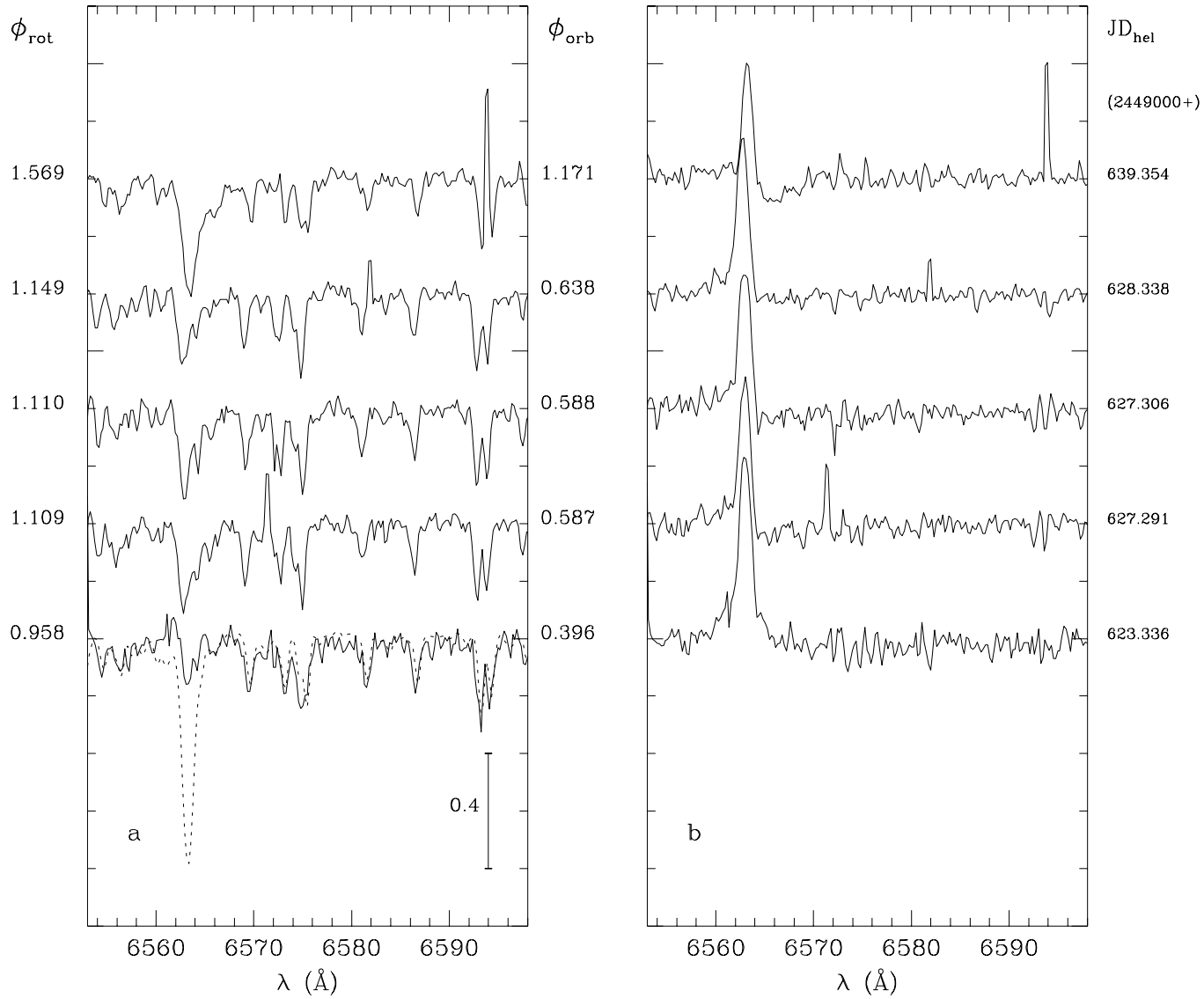

Fig. 9. **a** High resolution Hα spectra of HD 185510 in 1994 with superimposed the adopted standard ϵ Cyg (dotted line). **b** Residual Hα emission.

lation displayed by the Hα emission curve with respect to the photometric light curve, seems to indicate a clear spatial correlation of chromospheric active regions with the photospheric spotted regions, frequently observed in active RS CVn binaries (Catalano et al. 1996). We therefore assume that the Hα excess emission is mainly or completely due to chromospheric emission plages as also indicated by the Mg II emission seen at all orbital phases (Balona et al. 1987).

4.1. The evolutionary stage of the hot component

Jeffery & Simon (1997) concluded that on the basis of the Ly-α solution HD185510B could be a helium dwarf because of the high gravity $\log g = 7.2$, while from the photometric solution it would be identified as a sdOB star. Our values of the mass, radius and effective temperature lead us to place HD185510B (Fig. 12) close to the lower boundary of the sdB stars (Heber 1986, Moehler et al. 1990) in the log T_{eff}–log g diagram. The subluminous B and OB stars are considered extended horizontal branch (EHB) stars, which behave like helium main sequence stars, whose mass is constrained around 0.5 $M_\odot$. This average value has been mainly defined by the analysis of EHB stars in NGC 6752 (Heber 1986). HD185510B would be the first sdB star whose mass has been unambiguously determined, but its value M=0.3 $M_\odot$ is significantly smaller than the typical sdB star mass. Mengel et al. (1976) suggested that the sdB stars might be formed in close binary systems if Roche lobe overflow occurs during the core helium flash.

The question of how helium dwarfs are formed was first addressed by Kippenhahn, Kohl & Weigert (1967), who followed the Roche lobe filling phase of a primary of 2 $M_\odot$ and a secondary of 1 $M_\odot$. The primary fills its Roche lobe for the first time after it has exhausted hydrogen at its center and has devel-

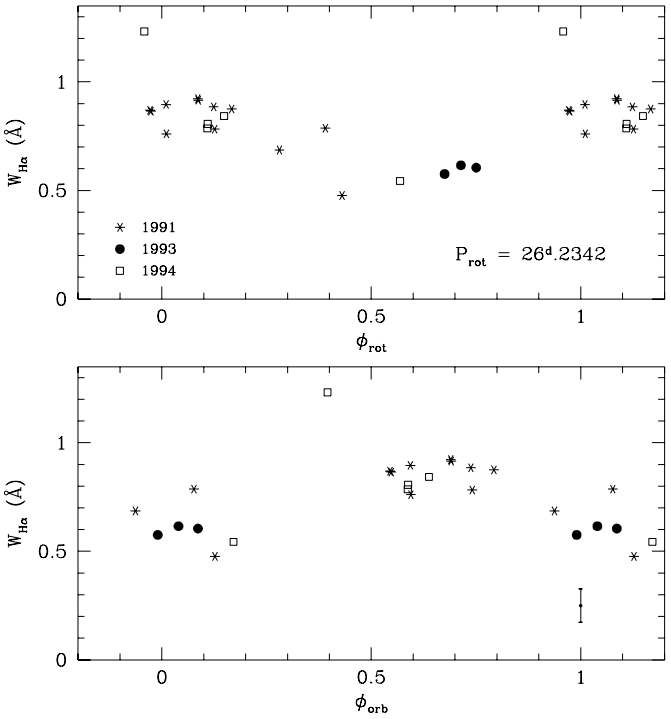

Fig. 10a and b. Net Hα equivalent width plotted against the orbital period (**a**) and the rotational period (**b**). Different symbols refers to 1991 and 1993 low resolution and 1994 high resolution data.

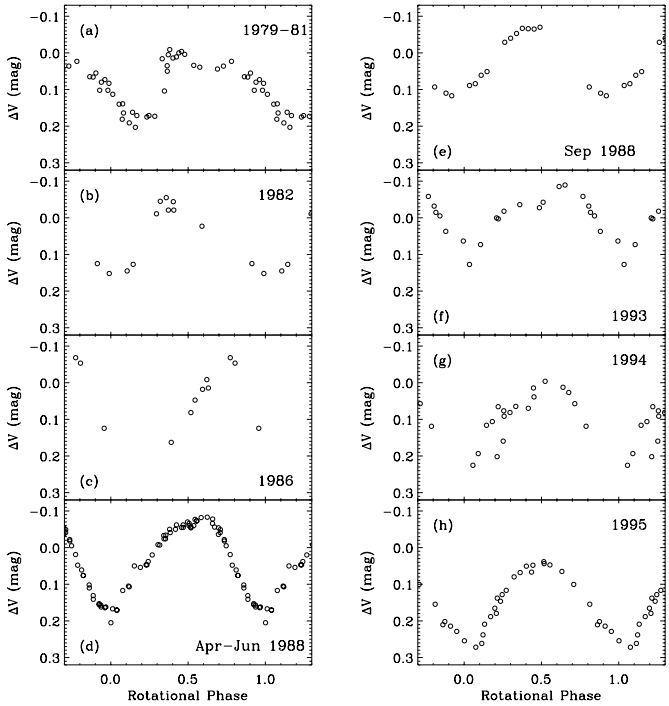

Fig. 11. V light curves of HD 185510 at various epoches. Phase are reckoned from the new photometric ephemeris JD$_{hel}$ = 2447315.826 + 26.2342×E

Table 4. Rotational V light curve parameters.

Session	Amp.	$< \Delta V >^*$	Φ_{min}	Ref.
1979-81	$0^m.18$	$0^m.09$	$0^P.20$	(a)
1982	$0^m.19$	$0^m.05$	$0^P.02$	(b)
1986	$0^m.2$:	$0^m.06$:	—	(c)
Apr-Jun 1988	$0^m.24$	$0^m.05$	$0^P.00$	(d)
Sep 1988	$0^m.18$	$0^m.02$	-$0^P.07$	(e)
1993	$0^m.18$	$0^m.01$	$0^P.03$	(f)
1994	$0^m.21$	$0^m.10$	$0^P.00$	(g)
1995	$0^m.22$	$0^m.16$	$0^P.04$	(h)

(a) Lloyd Evans & Koen (1987)
(b) Henry et al. (1982)
(c) Hooten & Hall (1990)
(d) Hooten & Hall (1990)
(e) Hooten & Hall (1990)
(f) Present work
(g) Present work
(h) Present work

* Mean magnitude level of V light curves

oped an electron degenerate helium core of mass ≈0.23 M$_\odot$. The final remnant dwarf would be only slightly more massive, by 0.03 M$_\odot$, than the helium core.

Moreover Iben & Tutukov (1986) discussed the formation and evolution of a helium-degenerate white dwarf of mass 0.3 M$_\odot$, i.e. just the mass of HD 185510B. Although the detailed model calculation is made for an initial mass of 1 M$_\odot$ it applies to any other model of initial mass less than 2.3 M$_\odot$, which forms an electron-degenerate helium core before the ignition of helium and which fills its Roche lobe for the first time when the core mass reaches a value of ∼ 0.3 M$_\odot$. The evolutionary track of the remnant, which undergoes two hydrogen flashes before reaching the final white dwarf cooling track passes close to the location of HD 185510B during the first cooling phase prior to the first flash (point D in Fig. 12, where the most relevant points of the 0.3 M$_\odot$ remnant evolution from Iben & Tutukov(1986) model are reported in the log T$_{eff}$–log g plane together with the location of sdB and sd stars). The evolution time to the first cooling phase is rather short, only about 3×10^6 years. This short time evolution, as already pointed out by Jeffery et al. (1992), is inconsistent with the evolution stage of the original secondary HD 185510A, which with an increased mass of 2.24 M$_\odot$ would reach the present giant stage of spectral class K0 III/IV in about 5.6 $\times10^8$ years (Iben 1967).

According to the various models the evolutionary characteristics of the system after the mass loss are almost entirely determined by the mass of the helium core at the onset of the mass loss phase. Where, in the case of HD 185510B, a degenerate helium core of 0.3 M$_\odot$ has been formed, as predicted by Iben & Tutukov (1986), or the core-helium ignition mass has been exceeded leading to a sdB star near the ZAEHB (Heber 1986, Moehler et al. 1990) it is difficult to state. The actual system parameters of HD 185510 and the condition that the primary has filled its Roche lobe for the first time when the helium core

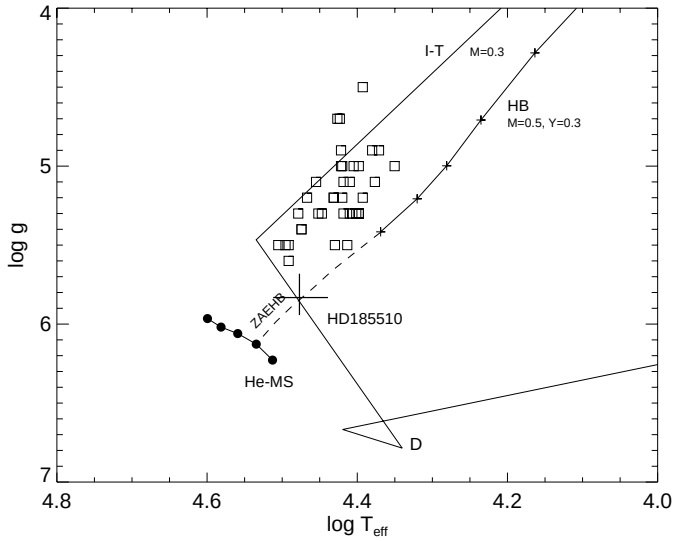

Fig. 12. The position of HD 185510B in the log T_{eff}–log g diagram (thick cross; solution for $E_{B-V} = 0^m.1$). The location of the zero-age horizontal branch for Y=0.3 and a helium core mass of 0.4691 (Sweigart 1987), an extrapolated extended horizontal branch (dashed line), the helium main sequence and the subdwarf OB stars adapted from Moehler et al. (1990) are indicated. The first part of the evolutionary track for a 0.296 $M_\odot$ helium star from Iben & Tutukov (1986) model [I-T] is represented by a thin line. The point D indicates the first shell helium flash.

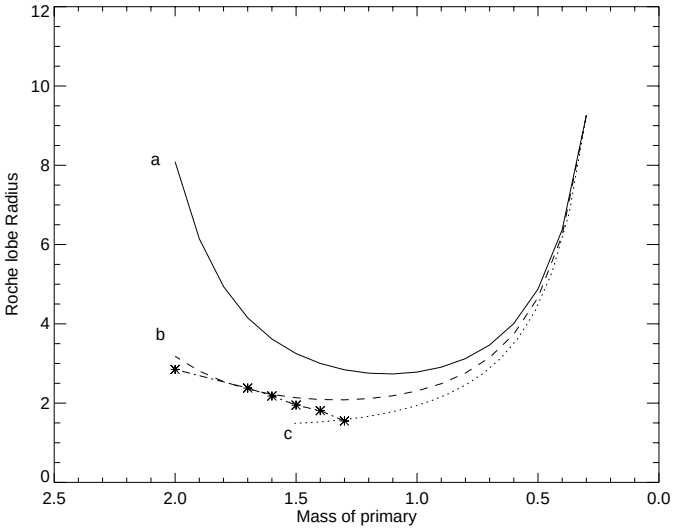

Fig. 13. Evolution of the Roche lobe radius of the original primary of HD 185510 during mass loss as a function of the remaining mass M_1. Curves are labelled as follows: a) conservative case, b) 10 % mass loss from the system, c) 14 % mass loss. The dash-dot line represent the radius values at the core-hydrogen exaustion for the various masses from Bertelli et al. (1986).

mass reached a value of $\sim 0.3\,M_\odot$ places important constraints on the initial parameters and on the mass loss behaviour.

Any interpretation of the evolutionary status of HD 185510B must also take into account the apparent evolved status of the original secondary component and of the dynamical evolution of the system as a consequence of the mass loss from the primary. In order to attempt to estimate the initial parameters of the system, we have made some simple calculations of the parameter evolution under different conditions of mass loss. Starting with the present period, mass and separation we have computed the initial system parameters using the formulae $P\,(M_1 + M_2)^2 = constant$ for mass loss from the system and $P\,(M_1 \times M_2)^3 = constant$ for mass transfer, which also imply angular momentum conservation. The Roche lobe radius, following Paczyński (1971), has been computed as:

$$\frac{R_R}{a} = 0.37771 + 0.20247 \log q + 0.01838\,(\log q)^2 + \quad (10)$$
$$+ \; 0.02275\,(\log q)^3$$

where *a* is the system separation and q the mass ratio.

In Fig. 13 we report the evolution of the Roche lobe radius as a function of the remaining mass of the original primary for the conservative case (only mass transfer) and mass transfer plus 10 % and 14 % mass loss. The comparison with the radius for the appropriate mass (Bertelli et al. 1986) at the core-hydrogen exhaustion (dash-dot line) shows that in the conservative case (curve a) Roche lobe overflow is expected during the shell Hydrogen burning, leading to a typical case B mass transfer, while the addition of only 10 % mass loss would lead to Roche lobe radius at the limit of case B overflow (curve b). A 14 % mass loss (curve c) produces a sizable shrinking of the orbit and therefore a Roche lobe radius smaller than that at the core hydrogen exhaustion, i.e. a case A overflow with a possible common envelope phase.

4.2. The asynchronism problem

As we have confirmed, the giant component of HD185510 is asynchronoulsy rotating, with a rotation period longer than the orbital one. Fekel & Eitter (1989) examined 114 chromospherically active binaries from the first edition of the Catalog of Active Binaries (Strassmeier et al. 1988) and found that 19 systems, i.e. about 17 %, including HD 185510 are definitely asynchronous. The fraction of asynchronous rotators increases with the orbital period, being between 86 % and 100 % for a period longer than 70 days. We have updated the Fekel & Eitter list with more recently determined rotation periods and noticed that about the 50 % of the asynchronous systems (11 out of 23) have rotation periods longer than the orbital one. We have investigated the dependence of the asynchronism on the various system parameters. Adopting the ratio $\omega_{orb}/\omega_{rot}$ as asynchronism parameter we have found that systems with a small mass function tend to have asynchronism parameter values > 1, i. e. rotation period longer than the orbital one, and values ≤ 1 for log f(m) ≥ -2. However, the best correlation is exhibited by the semimajor axis of primary star orbit, a_1, mesured in units of the star radius. Fig. 14, where the asynchronism ratio is plotted as a function of $\log(a_1/R_*)$, shows a linear dependence of the $\omega_{orb}/\omega_{rot}$ ratio on $\log(a_1/R_*)$, with stars of smaller a_1/R_* rotating slower than synchronous. These results can be interpreted

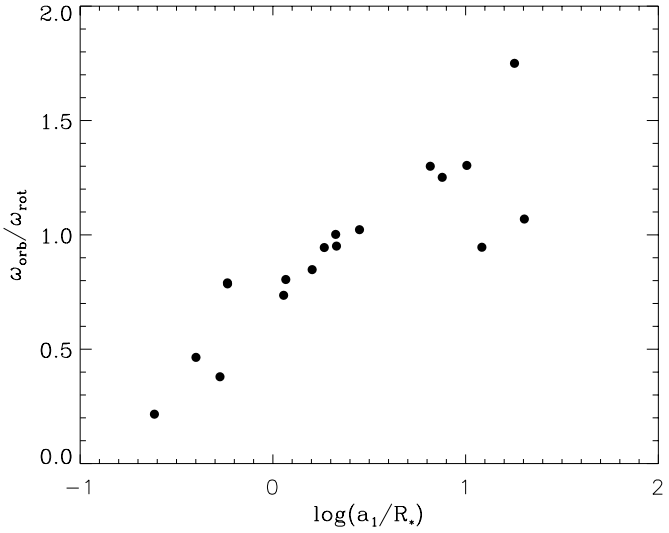

Fig. 14. Asynchronism parameter $\omega_{orb}/\omega_{rot}$ as a function of the semi-axis of the orbit of the more massive component in units of its radius

as follows. Small a_1 values indicate large mass ratios with the primary component of larger mass and consequently small mass function. In turn a small mass function means either a low mass companion or a long orbital period and therefore a large separation. The low mass of the companion and the large separation make the tidal effect inefficient to bring the giant primary to co-rotation in a time scale comparable to the evolution time of the star.

Habets & Zwaan (1989) have computed the rotation evolution of two systems similar to HD 185510, with low mass evolved secondary component, i.e. AY Cet and λ And. They show that during the evolution out of the ZAMS the angular rotation rate of the present primary decreases because of the increase of the moment of inertia and because of magnetic braking, as soon as the convective envelope sets in. The star can spin down to a frequency below the orbital frequency before the tidal interaction becomes strong enough to bring the star in synchronous rotation. They estimate the synchronization time scale according to Zahn (1977) and Campbell & Papaloizou (1983) as

$$\tau_{sync} = Fq^2[\frac{M_1 R_1}{L_1}]^{\frac{1}{3}}(\frac{a}{R_1})^6 \qquad (11)$$

where q=$\frac{M_1}{M_2}$ and F is a dimensionless structure constant. The observed dependence of the asynchronism coefficient on (a_1/R_*) is consistent with predictions, i.e. systems with lower mass function (longer orbital periods, larger separation) have on the average a larger asynchronism factor because the synchronization time is much longer.

Let us analyse now the rotational evolution of HD 185510A. Adopting the structure constant k given by Rutten & Pylyser (1988) and the present radius, we estimated that the moment of inertia between the main sequence, i.e. the end of mass accretion, and the present evolutionary status has increased by a factor of 80. This means that, if angular momentum is conserved, the star at the ZAMS spins with an equatorial velocity $v_{eq} \approx 260$ km/s, which is quite large for a normal 2.25 $M_\odot$ star. However, we have to consider that such high rotational velocity, at the end of the mass transfer, may be the result of accretion of about 1 $M_\odot$ of high angular momentum. If tidal interaction and magnetic bracking is included, according to the rotational evolution model for a 2 $M_\odot$ star by Habets & Zwaan (1989) HD 185510A should be already in co-rotation. The slight asynchronism observed for HD 185510A and the larger one for λ And (P_{rot}/P_{orb} = 2.7) seems to indicate that the time scale of the tidal interaction is significantly longer than predicted by Zahn (1977) and Campbell & Papaloizou (1983). Tassoul (1987) and Tassoul & Tassoul (1992) proposed a pure hydrodynamical mechanism for synchronization and circularization of binaries which predicts shorter time scales than the friction theory of Zahn (1977), therefore in more disagreement with our case.

If one has to give credit to Habets & Zwaan (1989) calculations, the still observed asynchronism of the K0 III component of HD 185510 should indicate that the mass transfer phase has ended only by a few 10^7 years and that the time scale evolution of the gaining mass stars is rather different from that of a single normal star, to which we have referred the evolutionary status of HD 185510A. In the case of short period binaries, as likely HD 185510 was before the beginning of the mass exchange (P= $1^d.2$ - $1^d.4$), the time scale for the mass transfer is so short that the companion could not be able to accrete all the mass, but will expand to form a giant envelope overflowing its Roche lobe (Iben & Tutukov 1986). The system passes through a common envelope phase, in which some matter, lost by the donor and of the order of 10 % according to the period evolution scenario of Fig. 13, is flowing out of the binary system. Unfortunately, there are not detailed models describing the very complex evolution of the common envelope phase and of the envelope expansion. In any case, the present temperature and luminosity of the remnant of the original primary star in HD 185510 do not sufficiently excite potential fluorescence of surrounding material to make it observable as a planetary nebula. However, the material may be cold enough to account for the large infrared excess observed by IRAS (Busso et al. 1988). This view would agree with the apparent evolution of the donor as a sdB in the EHB, or near the first hydrogen shell flash according to Iben & Tutukov (1986) model.

We would like to summarize the result of the present work stressing the following aspects:

Although HD 185510 is not a typical RS CVn, the giant K0 III component exhibits significant evidences of magnetic activity both at photospheric and chromospheric level.

Physical parameters of the two components have been improved through a more complete light curve and accurate solution.

The new values of the temperature and gravity classify HD 185510B as a B subdwarf about 10^7 years old. In order to comply with this short evolution time, the cooler giant component should have evolved through a common envelope out-of-equilibrium phase. A mass loss from the system of the order of 10-15 %, the signature of which could be the IR excess observed by IRAS (Busso et al. 1988), is then required.

Acknowledgements. This work has been supported by the Italian *Ministero dell' Università e della Riscerca Scientifica e Tecnologica*, the *Gruppo Nazionale di Astronomia* of the CNR and by the *Regione Sicilia* which are gratefully acknowledged. We acknowledge also dr. Franco Leone for the help in calculating the optical depth from Kurucz model atmosphere.

References

Antonopoulou E., 1983, A&A, 120, 85
Antonopoulou E., Williams P.M., 1984, A&A 135, 161
Amado P.J., Byrne P.B., 1996, A&A, in press
Balona L., 1987, South Africa Astron. Obs. Circ., No. 11,p.1
Balona L., Lloyd Evans T., Simon T., Sonneborn G., 1987, IBVS 3601
Barnes T.G., Evans D.S., Moffet T.J., 1978, MNRAS 183, 285
Bell R.A., Gustaffson B., 1989, MNRAS 236,653
Berriman G., De Campli W.M., Werner M.W., Hatchett S.P., 1983, MNRAS,205, 859
Blackwell D.E., Lynas-Gray A.E., 1994, A&A, 282, 889
Bertelli G., Bressan, A., Chiosi C., Angerer K., 1986 A&AS 66,191
Bidelman W.P., MacConnell D.J., 1973, AJ 78, 687
Bonanno G., Di Benedetto R., 1990, PASP 102, 835.
Busso M., Scaltriti F., Persi P., Ferrari-Toniolo M., Origlia L., 1988, MNRAS, 234,445
Campbell, C.G., Papaloizou J., 1983, MNRAS, 204,433
Catalano S., Marilli E., Trigilio C., 1988, NATO ASI Series Conf. 241, p.377, A.K. Dupree and M.T.VT. Lago eds.
Catalano S., Rodonò M., Frasca A., Cutispoto G., 1996, IAU Symp. N. 176 on "Stellar Surface Structure", K.G. Strassmeier & J.F. Linsky eds., Kluwer Publ., p. 403
Dragon J.N., Mutschlecner J.P., 1980, ApJ 239, 1045
Fekel F.C., Eitter J.J., 1989,AJ,97,1139
Fekel F.C., Henry G.W., Busby M.R., Eitter J.J., 1993, AJ 106, 2370
Fekel F.C., Simon T., 1985, AJ 90, 812
Fekel F.C., Moffet, T.J., Henry, G.W., 1986, ApJS,60,551
Frasca A., Catalano S., 1994, A&A 284, 883
Fraquelli D.A., 1984, ApJ 276, 243
Gray D.F., 1992, *The Observation and Analysis of Stellar Photospheres*, Cambridge University Press
Habets G.M.H.J., Zwaan C., 1989, A&A, 211, 56
Hall D.S., Montle R.G., Atkins H.L., 1975, Acta Astron. 25, 125
Heber U., 1986, A&A 155,33
Heber U., Hunger K., Jonas G., Kudritzki R.P., 1984, A&A 130, 119
Henry G.W., Murray S., Hall D.S., 1982, IBVS 2215
Hooten J.T., Hall D.S., 1990, ApJS 74, 225
Iben I., Ann. Rev. Astron. Astrophys, 1967, 5, 571
Iben, I.Jr., Tutukov, A.V. 1986, ApJ, 311,742
Jeffery C.S., Simon T., Lloyd Evans T., 1992, MNRAS 258, 64
Jeffery C.S., Simon T., 1997, MNRAS 286, 487
Kippenhahn R., Kohl K., Weigert A., 1967, ZsAp, 69,265
Kopal Z., 1959, *Close Binary Systems*, Chapman & Hall L.T.D., London, p. 190
Kurucz R.L., 1979, ApJS 40, 1
Lloyd Evans T., Koen M.C.J., Hultzer A.A., 1983, South Africa Astron. Obs. Circ., No. 7,p.82
Lloyd Evans T., Koen M.C.J., 1987, South Africa Astron. Obs. Circ., No. 11,p.21
Marilli E., Frasca A., Bellina-Terra M., Catalano S., 1995, A&A 295, 393
Mengel J.G., Norris J., Gross P.G. 1976, AJ, 204, 488
Milone E.F. 1976, ApJS 31, 93
Moehler, S., Heber, U., de Boer, K.S., 1990, A&A, 239,265
Montes D., Sanz-Forcada J., Fernández-Figueroa M.J., Lorente R., 1996, A&A 310, L29
Paczyński B. 1971, ARA&A 9,183
Roberts D.H., Lehár J., Dreher J.W., 1986, AJ 93, 968
Rutten, R.G.M., Pylyser E., 1988, A&A, 1991,227
Scargle J.D., 1982, ApJ 263, 835
Scargle J.D., Strecker D.W. 1979, ApJ 228, 838
Schmidt-Kaler, 1982, in: *Numerical Data and Functional Relationships in Science and Technology*, Landolt-Bornstein (eds.), p. 453
Schröder K.-P., Marshall K.P., Griffin R.E.M., 1996, A&A, 311, 631
Skumanich A., 1972, ApJ 171, 565
Strassmeier, K.G., Hall, D.S., Zeilik et al., 1988, A&AS, 72, 291
Sweigart A.V., 1987, ApJS 65, 95
Tassoul, J.L., 1987 ApJ 322,856
Tassoul, J.L., Tassoul M., 1992, ApJ, 395,259
Travis L.D., Matsushima S., 1968, ApJ 154, 689
Verma R.P., Ghosh S.K., Iyengar K.V.K., Rengarajan T.N., Tandon S.N.R.R., 1983, Astrophys. Space Sci., 97, 161
Zahn, J.P., 1977, A&A, 57,383